JPEDAV (2006) 27:676-683
DOI: 10.1361/154770306X153738
1547-7037/$19.00 ©ASM International

Phase-Field Investigation of Multicomponent Diffusion in Single-Phase and Two-Phase Diffusion Couples

R.R. Mohanty and Y. Sohn

(Submitted March 23, 2006; in revised form August 14, 2006)

Interdiffusion in hypothetical ternary single-phase and two-phase diffusion couples are examined using a phase-field model by numerically solving the nonlinear Cahn-Hilliard and Ginzburg-Landau equations. For diffusion couples assembled with a regular single-phase solution, constant chemical mobilities were used to examine the development of concentration profiles including uphill diffusion and zero-flux plane. Zero-flux plane for a component was observed to develop for a diffusion couple at the composition that corresponds to the activity of that component in one of the terminal alloys. Experimental thermodynamic parameters and composition-dependent chemical mobilities were used to examine the morphological evolution of the interphase boundary in solid-to-solid, two-phase diffusion couples. Instability at the interphase boundary was introduced initially (t = 0) by a small compositional fluctuation at the diffuse interface, and its evolution varied largely as a function of terminal alloys and related composition-dependent chemical mobility.

Keywords computation, interdiffusion, microstructure, multicomponent diffusion, phase field modeling, thermodynamics, zero flux planes

1. Introduction

During the past decade, the phase-field approach has been developed to model various phase transformations and microstructural developments in materials. Based on a diffuse interface theory,[1] the phase-field model can describe the microstructure at the mesoscale within the limit of the corresponding sharp interface description. Phase-field models have been extensively used to simulate phenomena such as solidification, spinodal decomposition, order-disorder transformations, grain growth, and coarsening in various material systems.[2] A phase-field model does not require the explicit tracking of the interface and accommodates the Gibbs-Thompson effect in its description.[2] Recently, Wu et al.[3,4] have demonstrated the capability of using the phase-field approach in predicting interdiffusion microstructures that develop in solid-to-solid diffusion couples. The applicability of a phase-field model[5-7] with an available thermodynamic and kinetic database is an additional benefit. This work reports the development of a phase-field model to assess and predict the development of concentration profiles and microstructures in multicomponent single-phase and multiphase solid-to-solid diffusion couples.

The work has been divided into two parts. First, the development of zero-flux planes in single-phase diffusion couples is examined with respect to the thermodynamic description. Specifically addressed in this work is the development of the zero-flux plane for a component and its relation to the activity of that component in one of the terminal alloys.[8-12] In the second part, the development of planar and nonplanar interfaces in two-phase, solid-to-solid diffusion couples[13,14] is examined based on initial interface perturbation and composition-dependent chemical mobility.

2. Formulation of Phase-Field Model

2.1 Thermodynamic Descriptions

Two models are used in this study, one for the simulation of single-phase diffusion couples, and the other for the simulation of two-phase diffusion couples. While the basic framework of the formulation is the same, formulation for the single-phase couples is characterized by a difference in the composition only, whereas that for the two-phase couples is characterized by a difference in composition as well as in structure.

For a ternary substitutional alloy containing elements A, B, and C, compositionally distinct phases are represented by the conserved composition field variable, the mole or atom fraction of an individual element [$c_i(x,t)$]. A nonconserved

This article was presented at the Multicomponent-Multiphase Diffusion Symposium in Honor of Mysore A. Dayananda, which was held during TMS 2006, the 135th Annual Meeting and Exhibition, March 12–16, 2006, in San Antonio, TX. The symposium was organized by Yongho Sohn of University of Central Florida, Carelyn E. Campbell of National Institute of Standards and Technology, Richard D. Sisson, Jr., of Worcester Polytechnic Institute, and John E. Morral of Ohio State University.

R.R. Mohanty and **Y. Sohn,** Advanced Materials Processing and Analysis Center, and Department of Mechanical, Materials and Aerospace Engineering, University of Central Florida, Orlando, FL. Contact e-mail: rmohanty@mail.ucf.edu.

field variable [$\eta(x,t)$] is used along with the composition variable to represent chemically as well as structurally distinct phases. Hereafter, η is referred to as the structure order (SO) parameter. The constraint of "conservation of mass" leads to:

$$\sum_{i=0}^{n} c_i(x,t) = 1.0,\; c(x,t) \geq 0 \qquad \text{(Eq 1)}$$

where, x and t are the position and time variables, respectively. Assuming that the lattice mismatch between different phases is negligible and externally applied force fields are absent, the total chemical free energy, F_{chem}, of the system can be expressed as the sum of the bulk chemical free energy, F_{bulk}, and the total interfacial energy, F_{int}. This total energy of the system is represented as the Helmoltz free energy F by using the extended Cahn-Hilliard free energy function:[1]

$$F_{\text{chem}} = F_{\text{bulk}} + F_{\text{int}} = F = N_V \int_V f(c_i, \eta) + \kappa_i(\nabla c_i)^2 + \kappa_\eta(\nabla\eta)^2, \quad i = A, B, C \qquad \text{(Eq 2)}$$

where, $f(c_A, c_B, \eta)$ is the bulk chemical free energy per atom of the homogeneous alloy, and N_V is the number of atoms per unit volume, which is assumed to be constant. In Eq 2, κ_i and κ_η are the gradient energy coefficients associated with the gradients of compositions of individual elements and η, respectively. The system evolves into its equilibrium condition by minimizing the total chemical free energy F. For single-phase diffusion couples in this study, a simple regular solution approximation for $f(c_i)$ is used[15] and is given by:

$$f(c_A, c_B, c_c) = RT\sum_i c_i \ln c_i + \sum_{i \neq j} \omega_{ij} c_i c_j \qquad \text{(Eq 3)}$$

where ω_{ij} are the binary regular solution parameters. In this study, it is assumed $\omega_{ij} = \omega_{ji} = 2.0$, which produces a single-phase solid solution without any miscibility gap.[16]

For two-phase diffusion couples, the free energy was derived by directly using the procedure described by Wu et al.[6] and Wang et al.[17] Here, the bulk chemical free energy is approximated by a Landau polynomial expansion as a function of composition and SO parameter given by:

$$f(c_A, c_B, \eta) = f^{\gamma}(c_A, c_B, 0) + \frac{A_2(c_A, c_B)}{2}\eta^2 + \frac{A_4(c_A, c_B)}{4}\eta^4 + \ldots \qquad \text{(Eq 4)}$$

The molar volume for the system is assumed to be constant, and component C is taken as the dependent variable. Thus, there are only two composition variables in the equation. $f^{\gamma}(c_A, c_B, 0)$ is the free energy of one phase (i.e., γ), which is calculated from the thermodynamic data available in the study by Huang and Chang.[18] The equilibrium free energy of the second phase (i.e., β) is obtained from Eq 4 by substituting the equilibrium SO parameter value $\eta_0(c_A, c_B)$, which is determined by:

$$\frac{\partial f(c_A, c_B, \eta)}{\partial \eta} = 0 \qquad \text{(Eq 5)}$$

$A_2(c_A, c_B)$ in Eq 4 is represented by a polynomial, which was obtained from Wu et al.[6]

2.2 Diffusion Equations

Kinetic equations were used to govern the temporal evolution of the composition variables and SO parameter following Huang et al.[15] and others.[19,20] The intrinsic flux of individual components relative to a lattice frame of reference is expressed using a linear and homogeneous function of the gradient in its chemical potential as:

$$J_i = -M_i \nabla \mu_i \qquad \text{(Eq 6)}$$

where, M_i is the intrinsic mobility of the component i, which is always positive value. The interdiffusion flux of each component $\tilde{J}_i$ in a laboratory frame of reference is given by Shewmon:[21]

$$\tilde{J}_i = J_i - c_i(J_A + J_B + J_C) \qquad \text{(Eq 7)}$$

where $\sum_i \tilde{J}_i = 0$. Substituting Eq. 6 into Eq. 7 yields:

$$\tilde{J}_i = -(1 - c_i)M_i\nabla\mu_i - c_i\sum_{j\neq i} M_j\nabla\mu_j, \text{ where } j = A, B, C \qquad \text{(Eq 8)}$$

Using the Gibbs-Duhem relation, $\sum_i c_i\nabla\mu_i = 0$ with Eq. 1 yields:

$$\begin{aligned}
\nabla\mu_A &= (1 - c_A)\nabla\mu_A^{eff} - c_B\nabla\mu_B^{eff} \\
\nabla\mu_B &= (1 - c_B)\nabla\mu_B^{eff} - c_A\nabla\mu_A^{eff} \\
\nabla\mu_C &= -c_A\nabla\mu_A^{eff} - c_B\nabla\mu_B^{eff}
\end{aligned} \qquad \text{(Eq 9)}$$

where, $\mu_A^{eff} = (\mu_A - \mu_C)$ and $\mu_B^{eff} = (\mu_B - \mu_C)$. Now the substitution of Eq 9 into Eq 8 gives:[15]

$$\tilde{J}_A = -[(1 - c_A)^2 M_A + c_A^2 M_B + c_A^2 M_C]\nabla\mu_A^{eff} + [c_B(1 - c_A)M_A + c_A(1 - c_B)M_B - c_A c_B M_C]\nabla\mu_B^{eff} \qquad \text{(Eq 10a)}$$

and

$$\tilde{J}_B = -[(1 - c_B)^2 M_B + c_B^2 M_A + c_B^2 M_C]\nabla\mu_B^{eff} + [c_B(1 - c_A)M_A + c_A(1 - c_B)M_B - c_A c_B M_C]\nabla\mu_A^{eff} \qquad \text{(Eq 10b)}$$

In this study, the authors have introduced the intrinsic mobility of each element as a linear function of its composition (i.e., $M_i = \beta_i c_i$, where β_i is the atomic mobility of individual element). Then, Eq 10 for the interdiffusion flux of individual components becomes:[15]

$$\tilde{J}_A = -[(1-c_A)^2\beta_A c_A + c_A^2\beta_B c_B + c_A^2\beta_C c_C]\nabla\mu_A^{eff} + [c_B(1-c_A)\beta_A c_A + c_A(1-c_B)\beta_B c_B - c_A c_B c_C \beta_C]\nabla\mu_B^{eff} \quad \text{(Eq 11a)}$$

and

$$\tilde{J}_B = -[(1-c_B)^2\beta_B c_B + c_B^2\beta_A c_A + c_B^2\beta_C c_C]\nabla\mu_B^{eff} + [c_B(1-c_A)\beta_A c_A + c_A(1-c_B)\beta_B c_B - c_A c_B c_C \beta_C]\nabla\mu_A^{eff} \quad \text{(Eq 11b)}$$

Equation 11 can be rewritten as:

$$\tilde{J}_A = -M_{AA}\nabla\mu_A^{eff} - M_{AB}\nabla\mu_B^{eff} \quad \text{(Eq 12a)}$$

and

$$\tilde{J}_B = M_{BA}\nabla\mu_A^{eff} - M_{BB}\nabla\mu_B^{eff} \quad \text{(Eq 12b)}$$

where M_{ij} are the effective chemical mobilities defined as:[15]

$$\begin{aligned} M_{AA} &= (1-c_A)^2\beta_A c_A + c_A^2\beta_B c_B + c_A^2\beta_C C_C \\ M_{BB} &= (1-c_B)^2\beta_B c_B + c_B^2\beta_A c_A + c_B^2\beta_C c_C \\ M_{AB} &= M_{BA} = -c_B(1-c_A)\beta_A c_A - c_A(1-c_B)\beta_B c_B + c_A c_B c_C \beta_C \end{aligned} \quad \text{(Eq 13)}$$

For simplicity in this study, it is assumed that M_{AB} and M_{BA} are equal in magnitude and sign, although this assumption may not be true for many ternary systems. For an inhomogeneous system, μ_i^{eff} is defined as the variational derivative of F with respect to c_i:

$$\mu_i^{eff} = \frac{\delta F}{\delta c_i} \; (i = A,B) \quad \text{(Eq 14)}$$

Using Eq 2 and 14, we arrive at the following equations:

$$\mu_A^{eff} = \frac{\partial f}{\partial c_A} - 2(\kappa_A + \kappa_C)\nabla^2 c_A - 2\kappa_C\nabla^2 c_B$$

$$\mu_B^{eff} = \frac{\partial f}{\partial c_B} - 2(\kappa_B + \kappa_C)\nabla^2 c_B - 2\kappa_C\nabla^2 c_A \quad \text{(Eq 15)}$$

The governing temporal equations can be expressed using the continuity equation by:

$$\frac{\partial c_i}{\partial t} = -\nabla \cdot \tilde{J}_i \;\; (i = A,B) \quad \text{(Eq 16)}$$

From Eq 11, 13, 15, and 16, the final governing equations to be solved are obtained as:

$$\frac{\partial c_A(x,t)}{\partial t} = \nabla\left[M_{AA}\nabla\left(\frac{\partial f}{\partial c_A} - 2\kappa_{AA}\nabla^2 c_A - 2\kappa_{AB}\nabla^2 c_B\right)\right] + \nabla\left[M_{AB}\nabla\left(\frac{\partial f}{\partial c_B} - 2\kappa_{AB}\nabla^2 c_A - 2\kappa_{BB}\nabla^2 c_B\right)\right] \quad \text{(Eq 17a)}$$

and

$$\frac{\partial c_B(x,t)}{\partial t} = \nabla\left[M_{BA}\nabla\left(\frac{\partial f}{\partial c_A} - 2\kappa_{AA}\nabla^2 c_A - 2\kappa_{AB}\nabla^2 c_B\right)\right] + \nabla\left[M_{BB}\nabla\left(\frac{\partial f}{\partial c_B} - 2\kappa_{AB}\nabla^2 c_A - 2\kappa_{BB}\nabla^2 c_B\right)\right] \quad \text{(Eq 17b)}$$

where, $\kappa_{AA} = \kappa_A + \kappa_C$, $\kappa_{BB} = \kappa_B + \kappa_C$, and $\kappa_{AB} = \kappa_{BA} = \kappa_C$.

2.3 Evolution of Structure Order Parameter

The evolution of the nonconserved field variable η is described by a relaxation equation that is often called the time-dependent Ginzburg-Landau equation or the Allen-Cahn equation:[22]

$$\frac{\partial \eta(x,t)}{\partial t} = -M_\eta \frac{\delta F}{\delta \eta} \quad \text{(Eq 18)}$$

and

$$\frac{\delta F}{\delta \eta} = \frac{\partial f}{\partial \eta} - 2\kappa_\eta \nabla^2 \eta \quad \text{(Eq 19)}$$

where, $M\eta$ is the relaxation constant that characterizes the interface mobility. Combining Eq 18 and 19 yields:

$$\frac{\partial \eta(x,t)}{\partial t} = -M_\eta\left[\frac{\partial f}{\partial \eta} - 2\kappa_\eta \nabla^2 \eta\right] \quad \text{(Eq 20)}$$

2.4 Initial Interface Perturbation for Multiphase Diffusion Couples

A random fluctuation, $\xi(x,t)$, was incorporated to introduce compositional fluctuations at the γ/β diffused interface for multiphase diffusion couples at $t = 0$ (i.e., not sustained) using $\xi(x,t)$ as given by Cook:[23]

$$\frac{\partial C_i}{\partial t} = \sum_j \nabla M_{ij}^k \nabla \frac{\delta F}{\delta C_i} + \xi(x,t) \;\; \text{where} \;\; \langle \xi(x,t) \rangle = 0 \quad \text{(Eq 21)}$$

where x and t are position and time variables, respectively. The fluctuation used is a Gaussian random noise with a mean of zero, and is uncorrelated in time. When used in Eq 21 at $t = 0$, the above condition makes sure that the alloy composition is conserved. The range of fluctuation varied from 0.005 to −0.005 of composition within the diffuse interface. It should be noted that the compositional fluctuation is not introduced everywhere in the system.

Table 1 Composition of alloys employed in phase-field simulation of solid-to-solid ternary diffusion couples

Alloy designation	Composition, atom fraction		
	A	B	C
α_5	0.225	0.325	0.450
α_7	0.010	0.550	0.440
θ_1	0.500	0.313	0.187
θ_2	0.336	0.364	0.300
θ_3	0.300	0.150	0.550
θ_4	0.365	0.235	0.400
γ_1	0.200	0.100	0.700
γ_2	0.300	0.130	0.570
β_1	0.100	0.350	0.550
β_2	0.050	0.450	0.500

Note: For alloys α_5 and α_7, components A, B, and C correspond to Cu, Ni, and Zn, respectively. Alloys θ_1, θ_2, θ_3, and θ_4 have been selected based on the activity of component B, $a_B = 0.6682$, $a_B = 0.6682$, $a_B = 0.4599$, and $a_B = 0.5641$, respectively, in light of the development of zero-flux planes.

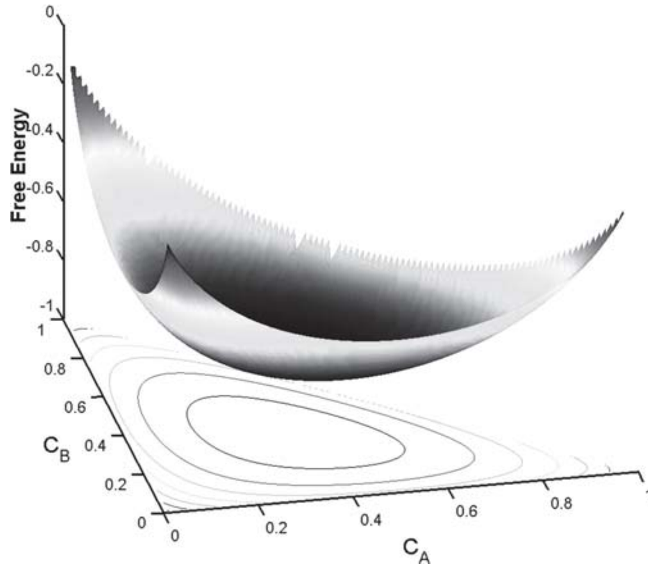

Fig. 1 Free energy surface with energy contours for a single-phase solution without any miscibility gap in the A-B-C ternary alloy

2.5 Numerical Implementation

Equations 17 and 20 were solved by using an explicit central finite-difference scheme. The system was divided into a 256 × 256 mesh, and the mesh size was equal to the dimensionless number 1.0 on both the *x* and *y* coordinates. The dimensionless time step used in the simulation was 10^{-5}. The work presented in this study is based on nondimensional numbers. The length scale represented by the *x*-axis does not represent any real dimension in this study. However, by assigning a unit to the mobility used, one can easily obtain results based on physical dimensions, although this may take a longer time to compute. Both the experimental and calculated concentration profiles that were developed can also be normalized by the Boltzmann parameter. For all multiphase diffusion couples, $\kappa_{AA} = \kappa_{BB} = -\kappa_{CC} = 0.75$, so that morphological variation is not a result of the variation in gradient energy coefficients for the diffusion couples studied.

Table 2 Chemical mobilities employed on either side of the solid-to-solid ternary diffusion couples examined in this study

Diffusion couple	Chemical mobility	LHS	RHS
α_5 (LHS) vs. α_7 (RHS)	M_{BB}	3.44	4.58
	M_{BC}	–0.05	0.62
	M_{CB}	26.45	15.25
	M_{CC}	23.9	9.73
θ_1 (LHS) vs. θ_2 (RHS)	M_{BB}	1.1	2.0
	M_{BC}	–0.8	–3.0
	M_{CB}	–1.2	–3.0
	M_{CC}	1.9	6.0
θ_3 (LHS) vs. θ_4 (RHS)	M_{BB}	0.2	0.5
	M_{BC}	–0.2	–0.8
	M_{CB}	–0.8	–0.1
	M_{CC}	8.1	6.8

Note: LHS, left-hand side; RHS, right-hand side

3. Single-Phase Ternary Diffusion Couples

In the current study, the authors have tried to predict the concentration profiles and diffusion paths in single-phase solid-to-solid diffusion couples. The composition of single-phase alloys used in this study is listed in Table 1, and chemical mobilities that were assumed to be constant on either side of the diffusion couple are listed in Table 2. The chemical mobilities are dimensionless and were chosen based on the average ternary interdiffusion coefficients determined from experimental concentration profiles[24] or randomly. Appropriate use of the kinetic parameters with a simple regular solution model allowed the prediction of concentration profiles that are commonly observed in ternary diffusion, including uphill diffusion and zero-flux planes. Figure 1 shows the free-energy surface with energy contours used for the regular solution model with $\omega = 2.0$. As an example, simulated and experimental concentration profiles from the Cu-nickel (Ni)-Zn diffusion couple, α_5 versus α_7 annealed at 775 °C for 48 h,[25] is presented in Fig. 2.

The regular solution presented in Fig. 1 was used to calculate[15] the isoactivity lines of component B in a hypothetical ternary system containing components A, B, and C. The development of concentration profiles into two single-phase diffusion couples was simulated with respect to the isoactivity of element B. For the couple θ_1 versus θ_2, compositions of both terminal alloys lie on one isoactivity line, whereas for θ_3 versus θ_4 the compositions of terminal alloys lie on two slightly different isoactivity lines, as presented in Fig. 3 and 4, respectively. Diffusion paths of the couples θ_1 versus θ_2 and θ_3 versus θ_4 on ternary isotherms are shown in Fig. 3(a) and 4(a), respectively. Though an

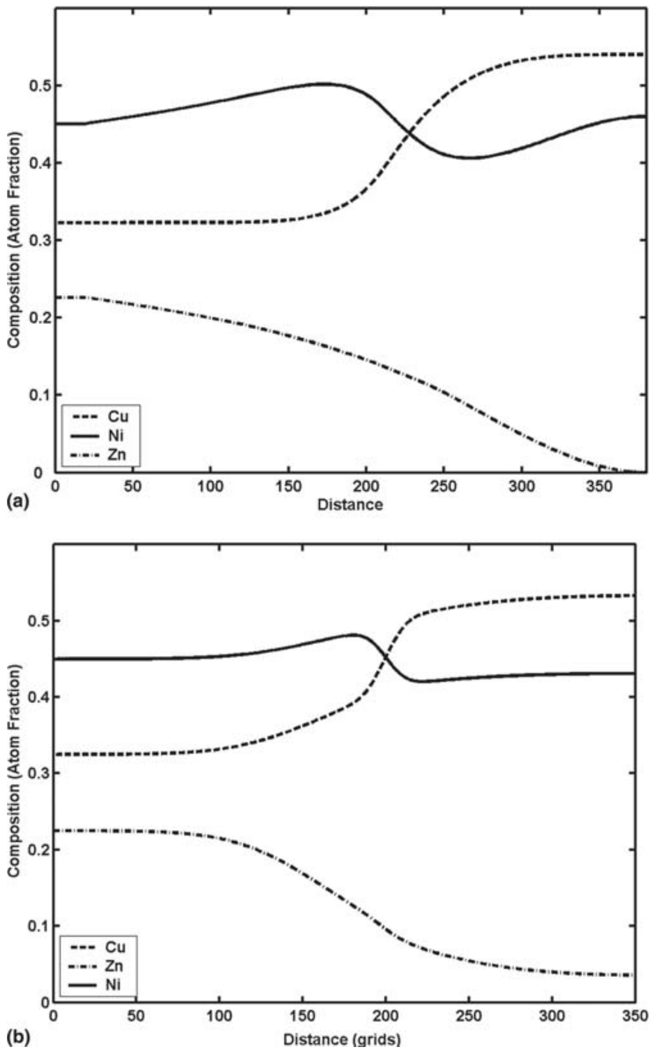

Fig. 2 (a) Experimental and (b) simulated concentration profiles of the solid-to-solid diffusion couple α_5 versus α_7

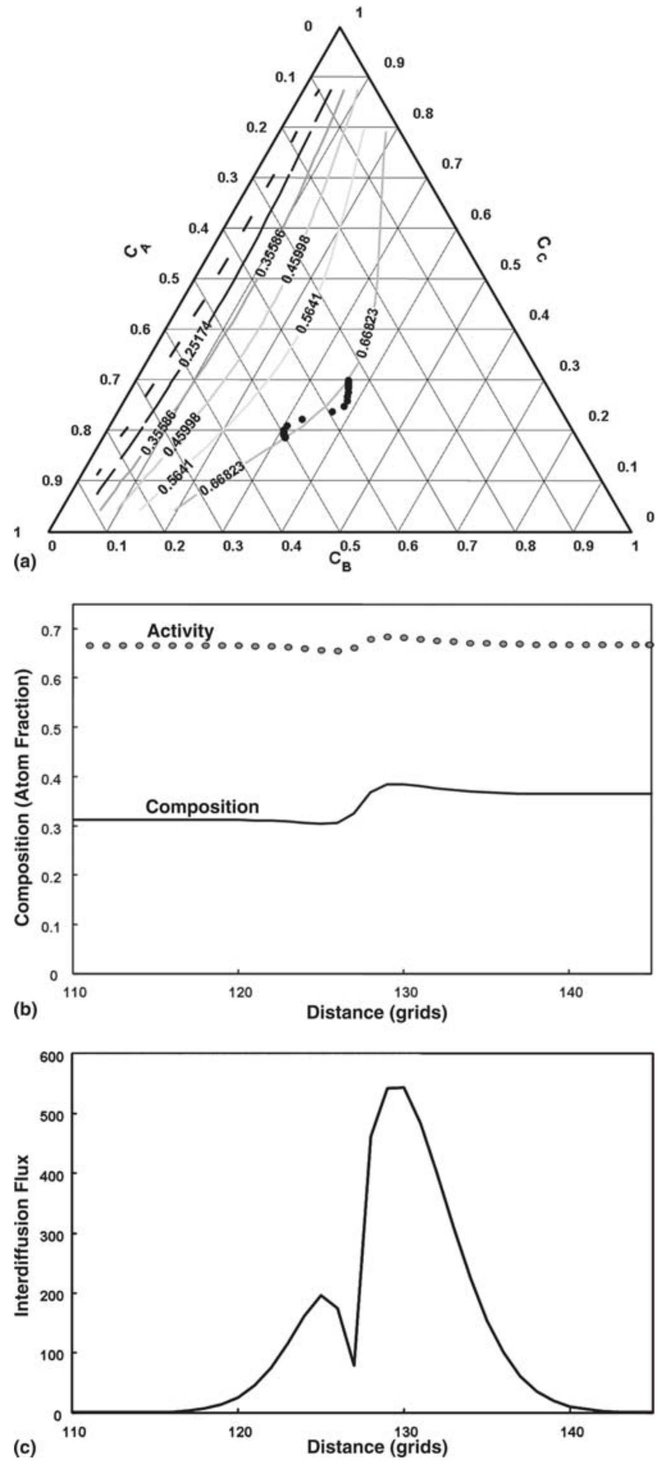

Fig. 3 (a) Diffusion path, (b) profiles of concentration and activity for component B, and (c) interdiffusion flux of component B simulated from diffusion couple θ_1 versus θ_2. The activity of B in both terminal alloys is the same at 0.6682. No zero-flux plane is observed, although an uphill diffusion for component B is observed.

uphill diffusion in the profiles of concentration and activity for component B was observed, as presented in Fig. 3(b) and 4(b), a zero-flux plane was only observed for the couple θ_3 versus θ_4. The activity of component B at the zero-flux plane composition (0.34A-0.235B-0.425C) corresponds to the activity of component B in the terminal alloy ($a_B = 0.5641$) on the right-hand side of Fig. 4(b). The simulated results for the couple θ_3 versus θ_4 agrees with the experimentally observed phenomena[8-10] that a zero-flux plane occurs at the composition where the diffusion path intersects the isoactivity line that extends from a terminal alloy. Occurrence of the zero-flux plane and its detailed relationship with thermodynamic and kinetic parameters are currently being examined systematically using the phase-field approach.

4. Two-Phase Diffusion Couples and Interface Morphology

To examine the morphological evolution of the interface between two-phase ternary diffusion couples, say γ versus β, the free-energy formulation given in Eq 4 was used. The free energy of the γ phase was derived from the thermodynamic database available for the Ni-Cr-Al system at

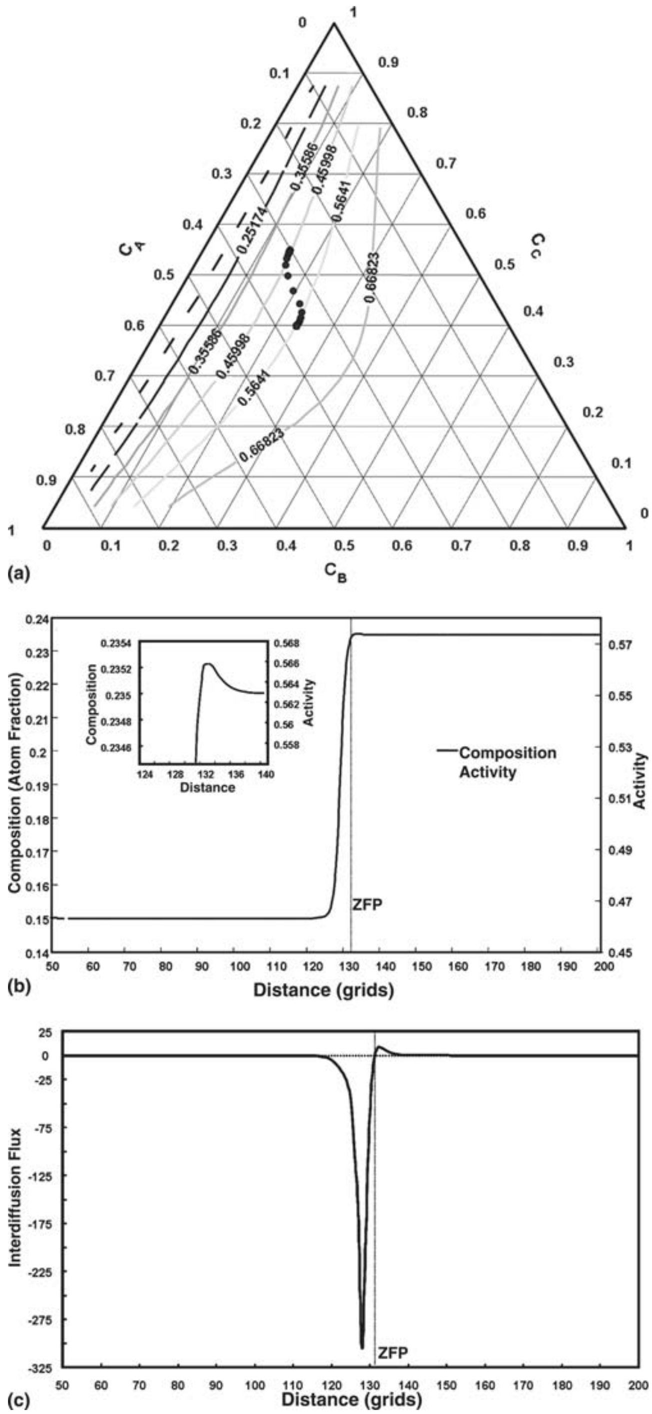

Fig. 4 (a) Diffusion path, (b) profiles of concentration and activity for component B, and (c) interdiffusion flux of component B simulated from diffusion couple θ_3 versus θ_4. The activities of component B in θ_3 and θ_4 alloys are 0.4599 and 0.5641, respectively. A zero-flux plane is observed with an uphill diffusion for component B. The activity of B at the zero-flux plane composition is 0.5641.

1200 °C.[18] Also, composition-dependent chemical mobilities, M_{ij}, based on Eq 13 were used in these simulations from constant atomic mobilities ($\beta_A = 2.0$, $\beta_B = 1.2$, and

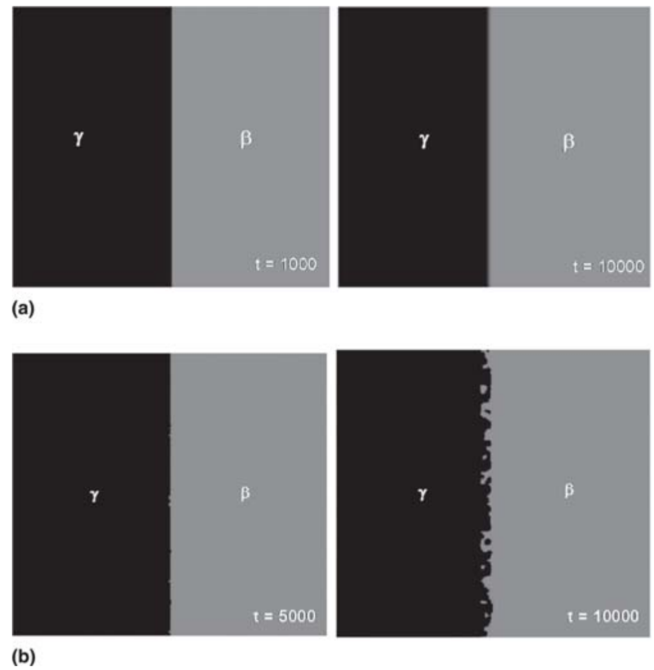

Fig. 5 Morphological evolution of the γ-β interface (a) with no initial fluctuation and (b) with initial fluctuation in the solid-to-solid, two-phase diffusion couple γ_1 versus β_1 with the same terminal alloy compositions. A nonplanar interface is observed to develop with the initial fluctuation.

$\beta_C = 6.0$). The authors first conducted two two-phase diffusion couple simulations: the first simulation was carried out without using any compositional fluctuations; and the second simulation was carried out with a uniform random fluctuation[23] across the interfacial region only in the first step of time iteration to introduce compositional perturbations into the system. Small random fluctuations that were introduced into the system did not result in the nucleation of precipitates or other phases. Each simulation is started with an initial homogeneous composition as determined by the thermodynamic equilibrium calculations. The terminal alloy compositions used in this study are provided in Table 1. The gradient energy terms used in this study for all diffusion couples are equal so that the variation in morphological development is not a result of the gradient energy variation from couple to couple. Equilibrium values of SO parameters ($\eta = 0$ for γ and $\eta = \eta_{eq}$ for β) for both the phases are used, and microstructures are presented with time snapshots using a gray-scale representation of the local values of η. In Fig. 5, the darker region in the microstructure corresponds to the γ phase ($\eta = 0$), and the brighter region corresponds to the β phase ($0 < \eta = \eta_{eq} < 1.0$). The results show that, without the introduction of perturbation, the γ-β interface moves parabolically and remains planar. With perturbation introduced at the interface at $t = 0$ only, the γ-β interface can become nonplanar.

Figure 6 presents the resulting microstructure from diffusion couples of different terminal alloy compositions, which have been subjected to the same fluctuation to study the effect of composition-dependent chemical mobilities on

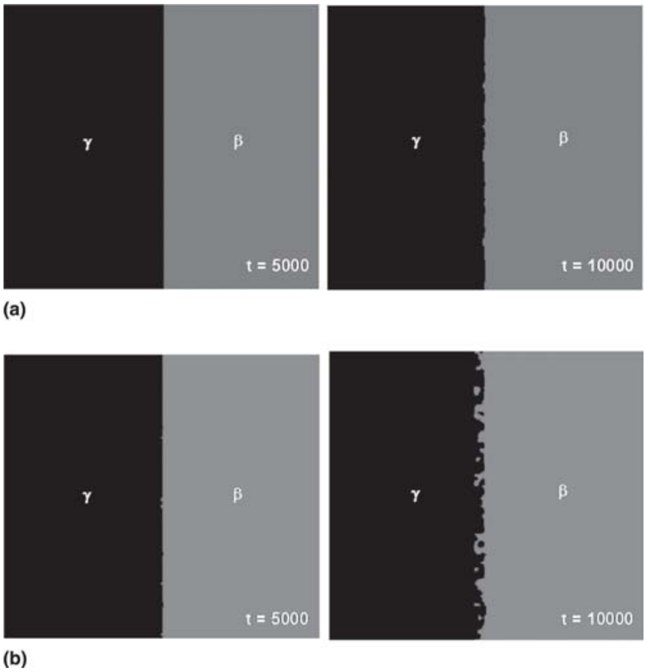

Fig. 6 Morphological evolution of γ-β interface in solid-to-solid diffusion couples: (a) γ_1 versus β_1; and (b) γ_2 versus β_2. The magnitude of the initial fluctuation is the same for both couples, while the terminal alloy compositions and composition-dependent chemical mobility vary.

the morphological evolution of the interface. It is observed that the initial terminal alloy compositions, and thus the composition-dependent chemical mobility, have a pronounced effect on the morphological evolution of the γ-β interface: planar in Fig. 6(a) versus nonplanar in Fig. 6(b). The morphological evolution of solid-to-solid multiphase diffusion couples is systematically being investigated as a function of the composition dependence of atomic and chemical mobility, which is determined by terminal alloy compositions.

5. Summary

A phase-field model was developed and used to simulate the development of concentration profiles and interface morphology observed in solid-to-solid ternary diffusion couples. Using a simple regular solution model, and constant chemical mobilities, the development of concentration profiles including uphill diffusion and zero-flux planes were simulated. A zero-flux plane for a component can be observed to develop at the composition that corresponds to the intersection of the diffusion path and the isoactivity line drawn from one of the terminal alloys. We also demonstrated that the terminal alloy compositions, and thus the composition-dependent chemical mobility, play an important role in the morphological evolution of the interphase boundary in solid-to-solid, two-phase diffusion couples.

Acknowledgments

This work is supported by a National Science Foundation CAREER Award under grant DMR-0238356. The authors would also like to express their appreciation to Dr. Carelyn Campbell, Dr. William J. Boettinger, Dr. James Warren, and Mr. Jonathan Guyer at the National Institute of Standards and Technology for technical assistance.

References

1. J.W. Cahn and J.E. Hilliard, Free Energy of a Nonuniform System. I. Interfacial Free Energy, *J. Chem. Phys.,* 1958, **28**(2), p 258-267
2. L.Q. Chen, Phase-Field Model for Microstructure Evolution, *Annu. Rev. Mater. Res.,* 2002, **32,** p 113-140
3. K. Wu, J.E. Morral, and Y. Wang, A Phase Field Study of Microstructural Changes Due to The Kirkindal Effect in Two-phase Diffusion Couples, *Acta Mater.,* 2001, **49,** p 3401-3408
4. K. Wu and Y. Wang, Predicting Interdiffusion Microstructures Using the Phase Field Approach, *Elevated Temperature Coatings: Science and Technology IV,* N. Dahorte, J. Hampikian, J. Morral, ed., The Minerals, Metals, & Materials Society, 2001
5. U. Grafe, B. Bottеger, J. Tiaden, and S.G. Fries, Coupling of Multicomponent Thermodynamic Database to a Phase Field Model: Application to Solidification and Solid State Transformations of Superalloys, *Scripta Mater.,* 2000, **42,** p 1179-1186
6. K. Wu, Y.A. Chang, and Y. Wang, Simulating Interdiffusion Microstructures in Ni-Al-Cr Diffusion Couples: A Phase Field Approach Coupled with CALPHAD Database, *Scripta Mater.,* 2004, **50,** p 1145-1150
7. Q. Chen, N. Ma, K. Wu, and Y. Wang, Quantitative Phase Field Modeling of Diffusion-Controlled Precipitate Growth and Dissolution in Ti-Al-V, *Scripta Mater.,* 2003, **50,** p 471-476
8. M.A. Dayananda and C.W. Kim, Zero-Flux Planes and Flux Reversals in Cu-Ni-Zn Diffusion Couples, *Metall. Trans. A,* 1979, **10A,** p 1333-1339
9. M.A. Dayananda, An Analysis of Concentration Profiles for Fluxes, Diffusion Depths, and Zero-Flux Planes in Multicomponent Diffusion, *Metall. Trans. A,* 1983, **14A,** p 1851-1858
10. C.W. Kim and M.A. Dayananda, Identification of Zero-Flux Planes and Flux Reversals in Several Studies of Ternary Diffusion, *Metall. Trans. A,* 1983, **14A,** p 857-864
11. C.W. Kim and M.A. Dayananda, Zero-Flux Planes and Flux Reversals in Cu-Ni-Zn Diffusion Couples at 775 °C, *Metall. Trans. A,* 1984, **15A,** p 649-659
12. J.G. Duh and M.A. Dayananda, Interdiffusion in Fe-Ni-Cr Alloys at 1100 °C, *Metall. Trans. A,* 1984, **15A,** p 649-659
13. R.D. Sisson Jr. and M.A. Dayananda, Diffusion Structures in Multiphase Cu-Ni-Zn Couples, *Metall. Trans.,* 1972, **3,** p 647-652
14. Y.H. Sohn, A. Puccio, and M.A. Dayananda, Interdiffusion Structures and Paths for Multiphase Fe-Ni-Al Diffusion Couples at 1000 °C, *Metall. Mater. Trans. A,* 2005, **36,** p 2361-2370
15. C. Huang, M. Olvera de la Cruz and B.W. Swift: "Phase Separation of Ternary Mixtures: Symmetric Polymer Blends," *Macromolecules,* 1995, **28,** p 7996-8005
16. C. Huang, M. Olvera de la Cruz, and P.W. Voorhees, Interfacial Adsorption in Ternary Alloys, *Acta Mater.,* 1999, **47**(17), p 4449-4459
17. Y. Wang, D. Banerjee, C.C. Su, and A.G. Khachaturyan, Field Kinetic Model and Computer Simulation of Precipitation of

$L1_2$ Ordered Intermetallics from F.C.C Solid Solution, *Acta Mater.,* 1999, **46**(9), p 2983-3001

18. W. Huang and Y.A. Chang, Thermodynamic Properties of the Ni-Al-Cr System, *Intermetallics,* 1999, **7,** p 863-874
19. S. Bhattacharyya, "Phase Separation in Ternary Alloys: A Diffuse Interface Approach," M.Sc. thesis, Indian Institute of Science, 2002
20. R.R. Mohanty, "A Diffuse Interface Model Study of Spinodal Decomposition Inside a Particle," M.E. thesis, Indian Institute of Science, 2002
21. P.G. Shewmon, *Diffusion in Solids,* McGraw-Hill Book Company, 1963
22. S.M. Allen and J.W. Cahn, A Microscopic Theory of Antiphase Boundary Motion and its Application to Antiphase Domain Coarsening, *Acta Metall.,* 1979, **27,** p 1085-1095
23. H.E. Cook, Brownian Motion in Spinodal Decomposition, *Acta Metall.,* 1970, **18,** p 297-306
24. M.A. Dayananda and Y.H. Sohn, A New Approach for the Determination of Interdiffusion Coefficients in Ternary Systems, *Metall. Mater. Trans. A,* 1999, **30**(3), p 535-544
25. R.D. Sission and M.A. Dayananda, Diffusional and Thermodynamic Interactions in the Cu-Ni-Zn System at 775 °C, *Metall. Trans. A,* 1977, **8,** p 1849-1856